Synthesis and Cation Distribution of the Spinel Cobaltites $Cu_xM_yCo_{3-(x+y)}O_4$ (M = Ni, Zn) Obtained by Pyrolysis of Layered Hydroxide Nitrate Solid Solutions

R. M. Rojas,* D. Kovacheva,† and K. Petrov†

Instituto de Ciencia de Materiales de Madrid, Consejo Superior de Investigaciones Científicas, Cantoblanco, 28049 Madrid, Spain, and Institute of General and Inorganic Chemistry, Bulgarian Academy of Sciences, 1113 Sofia, Bulgaria

Received May 26, 1999. Revised Manuscript Received August 23, 1999

A series of hydroxide nitrate solid solutions with a simple layered structure and general formula $Cu_mM_nCo_{2-(m+n)}(OH)_3NO_3$, (M = Ni, Zn) has been synthesized by double jet precipitation technique, from the corresponding aqueous metal nitrate solutions and NaOH. X-ray diffraction, infrared spectroscopy, and thermal analysis studies have shown that they are single phases which decompose thermally at about 200 °C, yielding the corresponding single-phase spinel-type oxides $Cu_xM_yCo_{3-(x+y)}O_4$ ($x = 3m/2$, $y = 3n/2$). The cation distribution in these complex spinels has been calculated on the basis of the tetrahedral and octahedral M−O distances determined by X-ray Rietveld refinement of their structures.

Introduction

Finely dispersed cobalt-containing oxide spinels $M_xCo_{3-x}O_4$ ($0 \le x \le 1$; M = Cu, Ni, Mg, Zn) have been known for a long time as catalysts for complete oxidation of hydrocarbons.[1,2] However, during the past decade the interest in them has increased considerably because these compounds are active in reactions involving oxidation of CO and hydrocarbons and the redox conversion of NO + CO mixtures to N_2 and CO_2. Their high activity, selectivity, and stability with respect to catalytic poisoning, which are comparable with those of noble metal-containing catalysts, offer the possibility for developing catalytic decomposers of harmful components in exhaust gases from internal combustion engines.[3−6] The spinel cobaltites of nickel, cobalt, or zinc are thermally unstable and cannot be prepared by a solid-state reaction between the corresponding oxide components.[7−10] However, they have been synthesized by using mild-condition techniques, e.g. low-temperature decomposition of mixed oxalates[11,12] or of specially designed hydroxide nitrate precursors.[13−16]

The crystal structure of hydroxide nitrates $M_2(OH)_3NO_3$ can be derived from that of brucite—$Mg(OH)_2$—in which one-quarter of the hydroxide ions are replaced by oxygen atoms from nitrate groups.[17] It is built up of alternating layers of metal−oxygen edge sharing octahedra, separated by a corrugated layer formed by the remaining nitrate oxygens.

It has been reported that the layered $Co_2(OH)_3NO_3$ is tolerant with respect to isomorphic replacement of Co^{2+} by other divalent ions over a large homogeneity range. Thus, the hydroxide nitrates of copper and cobalt, or nickel and cobalt form a continuous series of solid solutions $Cu_mCo_{2-m}(OH)_3NO_3$ and $Ni_mCo_{2-m}(OH)_3NO_3$ ($0 \le m \le 2$).[18,19] The hydroxide nitrates of zinc and cobalt form a continuous series of $Zn_mCo_{2-m}(OH)_3NO_3$ solid solutions with a maximum value of m of about 0.14−0.18. With m greater than 0.18, solid $Zn_mCo_{5-m}(OH)_8(NO_3)_2$ solutions are formed.[14] All these precursors decompose topotactically below 300 °C, yielding the corresponding $M_xCo_{3-x}O_4$ ($0 \le x \le 1$; M = Cu, Ni, Zn) binary spinel cobaltites.[14,20] Therefore, it is reasonable to expect that more complex $M_mM'_nCo_{2-(m+n)}(OH)_3NO_3$

† Bulgarian Academy of Sciences.

(1) Bliznakov, G. M.; Mehandjiev, D. R. *Kinet. Katal.* **198**7, *28,* 116. (in Russian).
(2) Mehandjiev, D. R.; Panayotov, D.; Khristova, M. *React. Kinet. Catal. Lett.* **1987**, *33*, 273.
(3) Terlecki-Baricevic, A.; Gribic, B.; Jovanovic, D.; Angelov, S.; Mehandjiev, D.; Marinova, C.; Kirilov-Stefanov, P. *Appl. Catal.* **1989**, *47*, 145.
(4) Dyakova, E.; Terlecki-Baricevic, A.; Mehandjiev, D.; Zhecheva, E.; Gribic, B. *React. Kinet. Catal. Lett.* **1991**, *43*, 521.
(5) Panayotov, D.; Khristova, M.; Mehandjiev, D. *J. Catal,* **1995**, *6*, 219.
(6) Panayotov, D.; Khristova, M.; Velikova, M. *Appl. Catal. B* **1996**, *9*, 107.
(7) Andrushkevich, T. V.; Boreskov, G. K.; Popovskii, V. V.; Plyasova, L. M.; Karakchiev, L. G.; Ostankovich, A. A. *Kinet. Katal.* **1968**, *9*, 1244 (in Russian).
(8) Baussart, H.; Le Bras, M.; Leroy, J. M. *C. R. Acad. Sci. Paris* **1977**, *C284*, 735.
(9) Ravindranathan, P.; Malesh, G. V.; Patil, K. C. *J. Solid State Chem.* **1987**, *66*, 20.
(10) Li, G. H.; Dai, L. Z.; Lu, D. S.; Peng, S. Y. *J. Solid State Chem.* **1990**, *89*, 267.
(11) Baussart, H.; Delobel, R.; Le Bras, M.; Leroy, J. M. *J. Chem. Soc., Faraday Trans.* **1979**, *75*, 1337.
(12) Peshev, P.; Toshev, A.; Gyurov, G. *Mater. Res. Bull.* **1989**, *24*, 33.
(13) Petrov, K.; Markov, L. *J. Mater. Sci.* **1985**, *20*, 1211.
(14) Petrov, K.; Markov; L.; Ioncheva, R. *J. Mater. Sci. Lett.* **1985**, *4*, 711.
(15) Markov, L.; Petrov, K. *React. Solids* **1986**, *1*, 319.
(16) Petrov, K.; Markov, L. Rachev, P. *React. Solids* **1987**, *3*, 67.
(17) Louer, M.; Louer, D.; Grandjean, D. *Acta Crystallogr.* **1973**, *B29*, 1696.
(18) Zotov, N.; Petrov, K. *Z. Krist.* **1990**, *190*, 235.
(19) Petrov, K.; Zotov, N.; Mircheva, E.; Garcia-Martinez, O.; Rojas, R. M. *J. Mater. Chem.* **1994**, *4*, 611.
(20) Petrov, K.; Markov, L.; Ioncheva, R.; Rachev, P. *J. Mater. Sci.* **1988**, *23*, 181.

10.1021/cm990331e CCC: $18.00
Published on Web 10/15/1999

Table 1. Composition and Lattice Parameters for the Hydroxyde Nitrate Precursors

precursor no.	composition	lattice parameter (Å)			unit cell volume (Å^3)
1	$Co_2(OH)_3NO_3$	$a_O = 5.50(5)$,	$b_O = 6.30(4)$	$c_O = 6.94(4)$	240(4)
2	$Cu_{0.05}$ $Ni_{0.21}Co_{1.74}(OH)_3NO_3$	$a_O = 5.52(1)$,	$b_O = 6.32(1)$	$c_O = 6.94(1)$	242(1)
3	$Cu_{0.20}Ni_{0.17}Co_{1.63}(OH)_3NO_3$	$a_O = 5.54(3)$,	$b_O = 6.34(2)$	$c_O = 6.94(2)$	244(2)
4	$Cu_{0.32}Ni_{0.11}Co_{1.57}(OH)_3NO_3$	$a_O = 5.57(1)$,	$b_O = 6.339(6)$	$c_O = 6.940(7)$	244.9(7)
5	$Cu_{0.03}Zn_{0.31}Co_{1.66}(OH)_3NO_3$	$a_O = 5.58(1)$,	$b_O = 6.324(9)$	$c_O = 6.94(1)$	245.1(7)
6	$Cu_{0.14}Zn_{0.20}Co_{1.66}(OH)_3NO_3$	$a_O = 5.52(2)$,	$b_O = 6.34(2)$	$c_O = 6.94(2)$	242.8(1)
7	$Cu_{0.26}Zn_{0.09}Co_{1.65}(OH)_3NO_3$	$a_O = 5.502(5)$,	$b_O = 6.327(4)$	$c_O = 6.931(4)$	241.3(3)

hydroxide nitrate precursors might convert into $M_xM'_y$-$Co_{3-(x+y)}O_4$ ($x = 3m/2$, $y = 3n/2$) spinels. In the present paper we report the synthesis and characterization of the ternary precursors $Cu_mM_nCo_{2-(m+n)}(OH)_3NO_3$ (M = Ni, Zn) and their corresponding $Cu_xM_yCo_{3-(x+y)}O_4$ spinel products obtained by thermolysis of the hydroxide nitrate solid solutions.

Experimental Section

Ternary hydroxide nitrate precursors $Cu_mM_nCo_{2-(n+m)}$-$(OH)_3NO_3$ (M = Ni, Zn) were prepared by the double jet precipitation method used in the synthesis of the hydroxide nitrates $M_mCo_{2-m}(OH)_3NO_3$ (M = Cu, Ni, Zn).[13−15] Equal volumes of 0.5 M NaOH and $Cu(NO_3)_2$ solutions were added simultaneously and at the same rate (3 mL min^{-1}) to a three-necked flask containing a boiling solution of 3 M $Co(NO_3)_2$ and $Ni(NO_3)_2$, or $Co(NO_3)_2$ and $Zn(NO_3)_2$, taken in selected ratios. The concentration of the $Cu(NO_3)_2$ solution was determined by the amount of Cu^{2+} ions desired in the solid phase. The process was performed with continuous stirring and ended after reaching about 75% precipitation of the total amount of the divalent metal cations. The precipitates were separated from the mother solutions by filtering, washed with distilled water and ethanol, and dried at 80 °C in air.

X-ray diffraction (XRD) measurements were carried out on DRON-3 (Co Kα) and Siemens D-501 (Cu Kα) powder diffractometers with a monochromatized diffracted beam. The patterns were scanned at a constant step of 0.02° (2θ) and 10 s/step counting time within the range 15° ≤ 2θ ≤ 140°. The unit cell parameters were calculated by the least-squares method.[21] The structure parameters of the obtained spinels were refined by the Rietveld method[22] (program DWB 9006PC[23]). A reference sample of Co_3O_4 obtained by thermolysis of $Co_2(OH)_3NO_3$ was used to estimate the quality of the refined data. The infrared (IR) spectra of vacuum-dried precursors, prepared as KBr disks, were recorded within the frequency range of 400−4000 cm^{-1} using a Bruker IFS25 FT spectrometer. Differential thermal analysis (DTA) and thermogravimetric (TG) curves of the precursors were taken between 20 and 1100 °C on Stanton STA 781 equipment in still air at a 10° min^{-1} heating rate, approximately 10 mg of sample was used in each run, and α-Al_2O_3 was used as the inert reference material. The elemental composition of the precursors after their dissolution in 0.1 M HCl was determined using a Perkin-Elmer ICP spectrometer.

Results and Discussion

Precursors. *X-ray Powder Diffraction*. The empirical formulas deduced from chemical analysis of all precursors and the refined unit cell parameters are given in Table 1. The parent compound of the precursors—$Co_2(OH)_3NO_3$—is monoclinic with $\beta = 90.0(9)°$ [18] (pseudorthorhombic, see Table 1). Since no monoclinic splitting of XRD lines was observed, the unit cell parameters of all samples were refined as pseudorthorhombic. As seen from the listed data, lattice parameters *b* and *c* remain practically constant with changing composition. Increasing the relative content of zinc causes an increase of the *a* parameter and the unit cell volume *V*, while increasing the relative nickel content has the opposite effect. If the formation of regular solid solutions is assumed, the observed trend can be explained by the fact that the zinc hydroxide nitrate has the largest (247 Å^3)[24] and the nickel hydroxide nitrate the smallest (234 Å^3)[25] unit cell volume.

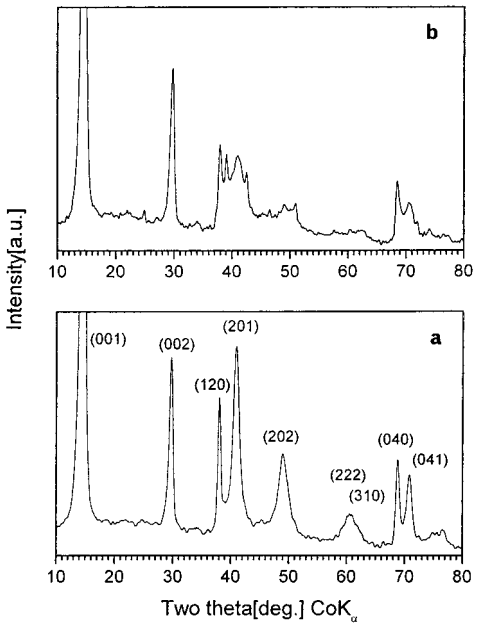

Figure 1. X-ray diffraction patterns recorded for (a) $Cu_{0.20}$-$Ni_{0.17}Co_{1.63}(OH)_3NO_3$ (precursor **3**) and (b) a mixture of 0.1 part $Cu_2(OH)_3NO_3$, 0.085 part $Ni_2(OH)_3NO_3$, and 0.815 part $Co_2(OH)_3NO_3$.

The X-ray diffraction pattern of $Cu_{0.20}Ni_{0.17}Co_{1.63}(OH)_3$-$NO_3$ (precursor **3**), that is typical for all precursors is shown in Figure 1a. It exhibits relatively sharp (00*l*) and (*hk*0) reflections, while those with indices (*hkl*) $l \neq 0$ are systematically broadened. This indicates the presence of positional and stacking disorder, inherent to the particular structural type of these compounds. Figure 1b shows the XRD pattern of a mechanical mixture of pure Cu, Ni, and Co hydroxide nitrates taken in a molar ratio of 0.20:0.17:1.63, respectively. This simple comparison demonstrates unambiguously that the precursor is a single-phase solid solution.

(21) Macicek, J. PDI—A Computer Program for Powder Data Interpretation, IAM, BAS, Sofia, 1988.
(22) Rietveld, H. M. *J. Appl. Cryst.* **1969**, *2*, 65.
(23) Sakhtivel, A.; Young, R. A. User Guide to Programs DBWS-9006 and DBWS-9006PC for Rietveld Analysis of X-ray and Neutron Powder Diffraction Patterns, School of Physica, Georgia Institute of Technology, Atlanta, 1991.
(24) Louer, M.; Grandjean, D.; Weigel, D. *Acta Crystallogr.* **1973**, *B29*, 1703.
(25) Gallezot, P.; Prettre, M. *Bull. Soc. Chim. Fr.* **1969**, *2*, 407.

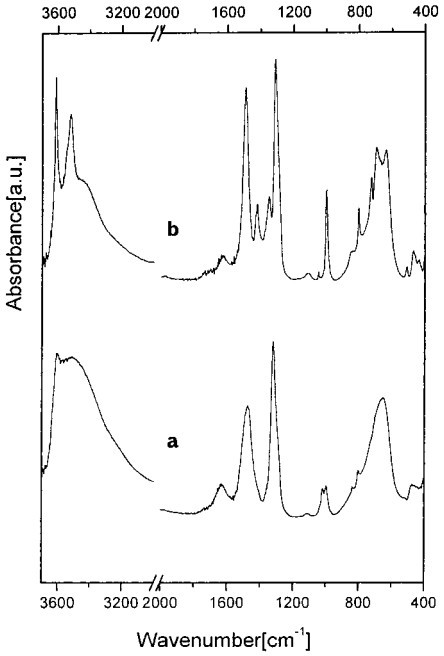

Figure 2. IR spectra of (a) $Cu_{0.20}$ $Ni_{0.17}Co_{1.63}(OH)_3NO_3$ (precursor **3**) and (b) a mixture of 0.1 part $Cu_2(OH)_3NO_3$, 0.085 part $Ni_2(OH)_3NO_3$ and 0.815 part $Co_2(OH)_3NO_3$.

Infrared Spectroscopy. Infrared spectroscopy can be used to characterize phase homogeneity and structural perfection of the samples in more details. In Figure 2a the spectrum of $Cu_{0.20}Ni_{0.17}Co_{1.63}(OH)_3NO_3$ (precursor **3**) is shown. Figure 2b shows the spectrum of a mechanical mixture of pure Cu, Ni, and Co hydroxide nitrates with the same overall composition. This simple comparison clearly shows that the spectrum of the ternary precursor is not a superposition of the spectra of its individual components $M_2(OH)_3NO_3$; M = (Cu, Co, Ni). In fact, spectrum a is similar to the spectra of the binary hydroxide nitrate solid solutions $Cu_xCo_{2-x}(OH)_3NO_3$[26] and $Ni_xCo_{2-x}(OH)_3NO_3$.[19] The NO_3 in-plane and out-of-plane bending vibrations (650−800 cm^{-1}) merge into one asymmetric broad complex band. This kind of broadening of IR absorption bands accompanied by a decrease in their intensities is typical of disordered solid solutions and mixed crystals. The degenerate E′ antisymmetric stretching vibration (1388 cm^{-1}) of the free NO_3 (D_{3h}) ion splits into ν_4 (1477 cm^{-1}) and ν_1 (1323 cm^{-1}) vibrations of the monodentate (C_s or C_{2v}) NO_3^- oxoanion. In general, the magnitude of splitting $\Delta = \nu_4 - \nu_1$ decreases with decreasing polarization ability (i.e. increasing ionic radius of the metal cation), being equal to 200, 180, and 84 cm^{-1} for Ni^{2+}, Co^{2+}, and Cu^{2+} pure compounds, respectively. The observed intermediate value of $\Delta = 154$ cm^{-1} for the particular spectrum shown in Figure 2a suggests that the degree of polarization of the NO_3 group is determined by the effective radius of the *mean* metal cation in the structure of the homogeneous solid solution formed. This is also confirmed by the monotonical compositional variation of Δ, observed in the spectra of all samples of the nickel and zinc precursor series. Another fact supporting the assumption that the ternary precursors are solid solutions is that the totally symmetric stretching vibration ν_2, which

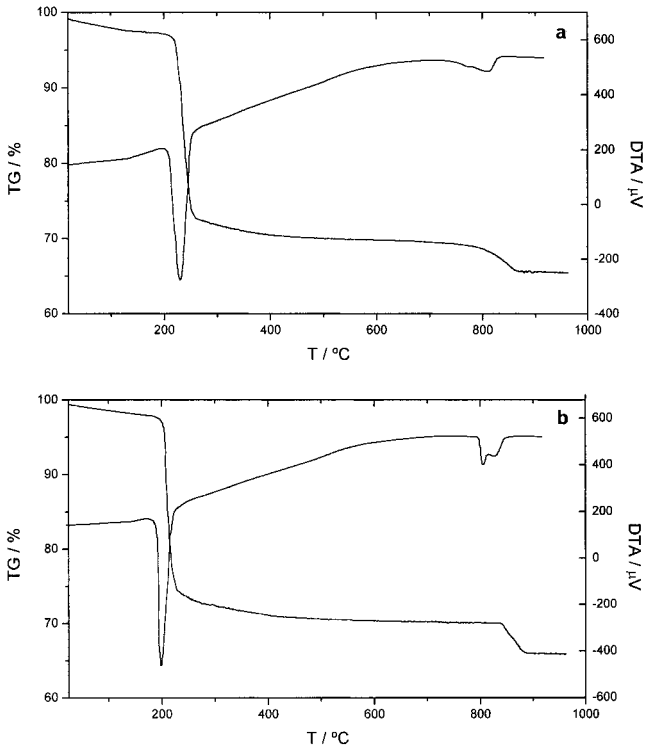

Figure 3. DTA and TG curves of (a) $Cu_{0.20}Ni_{0.17}Co_{1.63}(OH)_3NO_3$ (precursor **3**) and (b) $Cu_{0.14}Zn_{0.20}Co_{1.66}(OH)_3NO_3$ (precursor **6**).

appears as a single band at about 1000 cm^{-1} in the spectra of hydroxide nitrates containing one type of cation, splits in two close bands. Such splitting normally occurs when identical structural sites are occupied by different divalent cations.[26]

The stretching vibration ν' of the almost free OH^- group is assigned to the sharp band at 3610 cm^{-1}. The broad asymmetric band in the range 3250−3650 cm^{-1} stems from the additional hydrogen bonding between adjacent layers. Such broadening, indicative of the formation of a multicomponent solid solutions, has been also observed in other layered hydroxy salts.[27]

Thermal Analysis. DTA and TG curves recorded for $Cu_{0.20}Ni_{0.17}Co_{1.63}(OH)_3NO_3$ (precursor **3**) and $Cu_{0.14}Zn_{0.20}Co_{1.66}(OH)_3NO_3$ (precursor **6**), are presented in parts a and b of Figure 3, respectively. The thermal decomposition of all precursors takes place in a single step between 200 and 250 °C, as indicated by the endothermic effect observed in this temperature interval. At these temperatures the precursors are transformed into complex spinel products according to the reaction:

$$3Cu_mM_nCo_{2-(m+n)}(OH)_3NO_3 = 2Cu_{3m/2}M_{3n/2}Co_{3-3(m+n)/2}O_4 + 4.5H_2O\uparrow + NO\uparrow + 2NO_2\uparrow + 0.25O_2\uparrow \quad (1)$$

The weight loss determined for each precursor agrees well with that calculated for reaction 1 (Table 2). Data for $Co_2(OH)_3NO_3$ are included for comparison. Note that the temperature of decomposition is slightly higher for

(26) Zotov, N.; Petrov, K.; Dimitrova-Pankova, M. *J. Phys. Chem. Solids* **1990**, *51*, 1199.

(27) Delmas, C. *Proceedings of Symposium A2 on Solid State Ionics of the ICAM-91*; Balkanski, M., Takahashi, T., Tuller, H. L., Eds.; Elsevier Science Publishers B. V.: New York, **1992**; p 135.

Table 2. Temperatures (T_1, T_2, and T_3) and Weight Loss for the Endothermic Reactions Undergone by the Precursors and by the Spinel-type Oxide Products

precursor no.	T_1 (°C)	products composition	weight loss (%) calc	weight loss (%) found	T_2 (°C)	T_3 (°C)	products description	weight loss (%) calc	weight loss (%) found
1	192	Co_3O_4	30.46	30.28	900		CoO	6.64	6.62
2	238	$Cu_{0.07}Ni_{0.32}Co_{2.61}O_4$	30.40	29.94	858		CuO + $(Ni_{0.11}Co_{0.89})O$	3.61	4.01
3	240	$Cu_{0.29}Ni_{0.25}Co_{2.46}O_4$	30.36	30.00	812	850	CuO + $(Ni_{0.09}Co_{0.91})O$	4.82	4.61
4	236	$Cu_{0.48}Ni_{0.16}Co_{2.36}O_4$	30.28	29.86	833	854	CuO + $(Ni_{0.06}Co_{0.94})O$	5.52	5.4
5	210	$Cu_{0.04}Zn_{0.47}Co_{2.49}O_4$	30.18	29.47	841	878	CuO + ZnO + CoO	5.15	4.74
6	212	$Cu_{0.21}Zn_{0.30}Co_{2.49}O_4$	30.77	30.66	846	868	CuO + ZnO + CoO	4.02	4.30
7	220	$Cu_{0.39}Zn_{0.14}Co_{2.47}O_4$	30.22	29.74	848	866	CuO + ZnO + CoO	4.6	4.31

Table 3. Lattice Parameter *a* (Å), Oxygen Parameter *u*, Isotropic Displacement Parameters *B*(A), *B*[B], *B*(O) [Å²], Discrepancy Factors R_{wp}(%) and R_B (%), and Goodness of Fit *S* for the Spinel Products Obtained from Precursors 1−7

spinel composition	*a*	*u*	*B*(A)	*B*[B]	*B*(O)	R_{wp}	R_B	*S*
Co_3O_4	8.0798(3)	0.2655(2)	0.43(5)	0.44(3)	0.51(7)	5.80	4.80	1.08
$Cu_{0.07}Ni_{0.32}Co_{2.61}O_4$	8.1085(6)	0.2638(4)	0.40(6)	0.31(9)	0.50(9)	10.11	5.70	1.04
$Cu_{0.29}Ni_{0.25}Co_{2.46}O_4$	8.1161(6)	0.2641(4)	0.60(5)	0.51(8)	0.64(9)	9.25	4.90	1.01
$Cu_{0.48}Ni_{0.16}Co_{2.36}O_4$	8.1210(2)	0.2632(5)	0.66(7)	0.57(6)	0.68(8)	9.05	7.30	1.03
$Cu_{0.04}Zn_{0.47}Co_{2.49}O_4$	8.1117(8)	0.2649(5)	0.58(6)	0.55(5)	0.63(9)	10.10	5.15	1.01
$Cu_{0.21}Zn_{0.30}Co_{2.49}O_4$	8.1118(5)	0.2631(3)	0.47(7)	0.45(5)	0.58(9)	7.68	3.47	1.03
$Cu_{0.39}Zn_{0.14}Co_{2.47}O_4$	8.1150(4)	0.2627(3)	0.61(8)	0.63(5)	0.66(8)	7.30	5.17	1.03

$Cu_mM_nCo_{2-(m+n)}(OH)_3NO_3$ than for $Co_2(OH)_3NO_3$. Moreover, the zinc-containing hydroxide nitrates decompose at a temperature lower than that for nickel-containing compounds (Table 2). X-ray diffraction patterns recorded for the solid products formed at 300 °C correspond to cubic spinel-type oxides, and their lattice parameters are presented in Table 3. Between 300 and 800 °C, the thermogravimetric curves display a continuous and small weight loss (less than 2.5 wt %) due to the removal of excess oxygen, as has already been observed in the thermogravimetric curves of related compounds.[19] This effect is more evident in precursors **2**−**4**. Between 800 and 900 °C, DTA curves exhibit two endothermic peaks, which are accompanied by a weight loss. To ascertain the origin of these endothermic transformations, X-ray powder diffraction patterns were recorded on the solid products formed at the onset of the endothermic peaks (T_2 and T_3 in Table 2). The X-ray analysis data show that the first lower temperature peaks (T_2) correspond to segregation of CuO from the complex cobaltites, which transforms into a mixture of CuO and the binary $Ni_zCo_{3-z}O_4$ or $Zn_zCo_{3-z}O_4$ spinels. The second higher temperature peaks (T_3) correspond to the decomposition of $Ni_zCo_{3-z}O_4$ to (Ni,Co)O solid solutions, with a NaCl-type structure, or of $Zn_zCo_{3-z}O_4$ to a mixture of ZnO and CoO. This reaction sequence is explained by the well-known fact that the thermal stability of the cobaltites increases in the row as $CuCo_2O_4 < NiCo_2O_4 < ZnCo_2O_4$.[7,8] Calculated and experimental weight losses undergone by the spinel products are also presented in Table 2.

Spinel-type Oxide Products. *Rietveld Refinement.* The spinels $Cu_xNi_yCo_{3-(x+y)}O_4$ and $Cu_xZn_yCo_{3-(x+y)}O_4$ ($x = 3m/2$, $y = 3n/2$) obtained from thermal decomposition of the corresponding precursors in air at 300 °C for 4 h are single-phase black powdery substances with a specific surface area of about 40−47 $m^2\ g^{-1}$ (BET). Rietveld refinement of the X-ray powder diffraction data recorded for each spinel was carried out in the space group *Fd*3*m* [cationic positions, 8(a) and 16(d); oxygen positions, 32(e)] using atomic scattering factors for both neutral and ionized atoms. A pseudo-Voigt function was used as a profile approximation. The refined parameters were the zero position, the scale factor, the background parameters, the half-width parameters, the mixing parameter of the pseudo-Voigt function, the lattice parameter *a*, the oxygen position parameter *u*, and the individual isotropic displacement parameters *B*(A), *B*[B], and *B*(O) for the tetrahedral (A), octahedral [B], and oxygen (O) positions. Best fits were observed for parameters presented in Table 3. Figure 4a,b shows Rietveld plots for the spinels $Cu_{0.29}Ni_{0.25}Co_{2.46}O_4$ and $Cu_{0.21}Zn_{0.30}Co_{2.49}O_4$ obtained from thermal decomposition of precursors **3** and **6**, respectively.

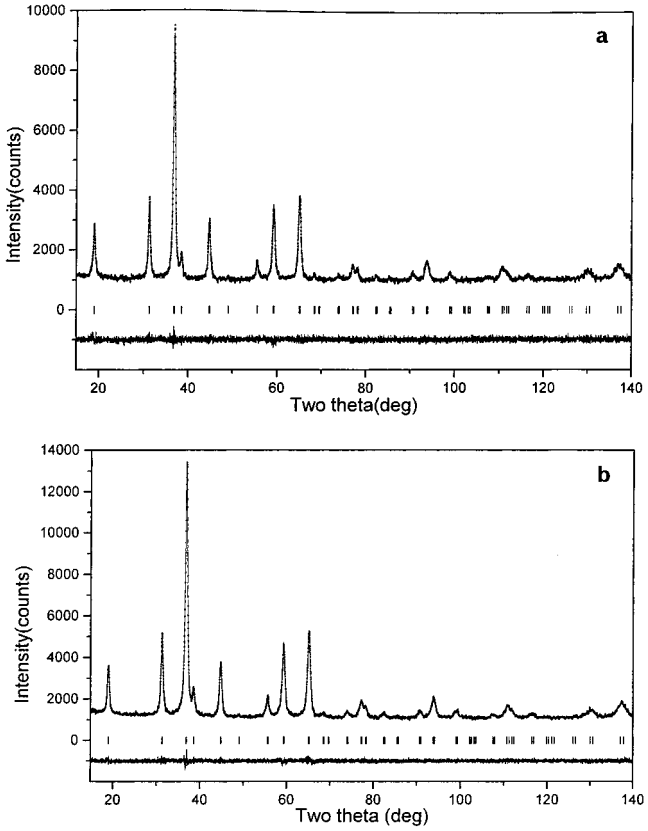

Figure 4. Rietveld plots of spinels: (a) $Cu_{0.29}Ni_{0.25}Co_{2.46}O_4$; (b) $Cu_{0.21}Zn_{0.30}Co_{2.49}O_4$, obtained from $Cu_{0.20}Ni_{0.17}Co_{1.63}(OH)_3NO_3$ (precursor **3**); and $Cu_{0.14}Zn_{0.20}Co_{1.66}(OH)_3NO_3$ (precursor **6**), respectively.

The small differences in the atomic scattering factors of the cations do not allow direct refinement of the

Table 4. Observed and Calculated Tetrahedral *L*(A) and Octahedral *L*[B] Bond Lengths (Å), and Proposed Structural Formulation for the $Cu_xM_yCo_{3-(x+y)}O_4$ (M = Ni, Zn) Spinels[a]

spinel composition	$L(A)_{obs}$	$L(A)_{calc}$	$L(B)_{obs}$	$L(B)_{calc}$	proposed structural formulation
Co_3O_4	1.966(2)	1.96	1.903(2)	1.91	$(Co^{2+})_A[Co^{3+}_2]_B$
$Cu_{0.07}Ni_{0.32}Co_{2.61}O_4$	1.960(4)	1.96	1.916(4)	1.92	$(Cu^{2+}_{0.07}Co^{2+}_{0.93})_A[Ni^{3+}_{0.32}Co^{3+}_{1.68}]_BO_4$
$Cu_{0.29}Ni_{0.25}Co_{2.46}O_4$	1.950(3)	1.95	1.924(3)	1.92	$(Cu^{2+}_{0.19}Co^{3+}_{0.1}Co^{2+}_{0.71})_A[Cu^{2+}_{0.1}Ni^{3+}_{0.25}Co^{3+}_{1.65}]_BO_4$
$Cu_{0.48}Ni_{0.16}Co_{2.36}O_4$	1.944(4)	1.94	1.929(4)	1.93	$(Cu^{2+}_{0.31}Co^{3+}_{0.16}Co^{2+}_{0.53})_A[Cu^{2+}_{0.17}Ni^{3+}_{0.16}Co^{3+}_{1.67}]_BO_4$
$Cu_{0.04}Zn_{0.47}Co_{2.49}O_4$	1.966(4)	1.96	1.915(4)	1.91	$(Zn^{2+}_{0.47}Co^{3+}_{0.04}Co^{2+}_{0.49})_A[Cu^{2+}_{0.04}Co^{3+}_{1.96}]_BO_4$
$Cu_{0.21}Zn_{0.30}Co_{2.49}O_4$	1.940(3)	1.94	1.927(3)	1.93	$(Zn^{2+}_{0.3}Cu^{2+}_{0.04}Co^{3+}_{0.17}Co^{2+}_{0.49})_A[Cu^{2+}_{0.17}Co^{3+}_{1.83}]_BO_4$
$Cu_{0.39}Zn_{0.14}Co_{2.47}O_4$	1.933(3)	1.93	1.933(3)	1.93	$(Zn^{2+}_{0.14}Cu^{2+}_{0.16}Co^{3+}_{0.23}Co^{2+}_{0.47})_A[Cu^{2+}_{0.23}Co^{3+}_{1.77}]_BO_4$

[a] Site occupancies for both tetrahedral (A) and octahedral [B] positions have been determined from eq 2.

cationic distribution in the investigated spinels.[28] Preliminary results obtained with fixed normal, inverse, and statistical models have shown that the type of cationic distribution for each composition does not affect the structure parameters a great deal. The lattice parameter *a* and the oxygen parameter *u* vary within the range of one standard deviation ($\Delta a \approx 0.0005$ Å, $\Delta u \approx 0.0004$). However, the *a* and *u* values vary from one spinel to another. In this case, at least semiquantitative, physically meaningful information about the cation distribution can be obtained by a comparison of the observed tetrahedral $L(A)_{obs}$ and octaherdral $L[B]_{obs}$ bond distances with their corresponding values calculated in the simplest linear form[29]

$$L(A)_{calc} = \sum_i x_i R(A)_i + 1.38$$

$$L[B]_{calc} = {}^1/_2 \sum_i x_i R[B]_i + 1.38 \quad (2)$$

where x_i stands for the partial site occupancy, $R(A)_i$ and $R[B]_i$ are the corresponding tetrahedral and octahedral ionic radii, and 1.38 Å is the value of the ionic radius of tetracoordinated O^{2-}. Calculations made with the so-called spinel ionic radii[29] (in Å) of Ni^{2+}(A), 0.565; Ni^{2+}-[B], 0.69; Co^{2+}(A), 0.58; Co^{2+}[B], 0.72; Co^{3+}(A), 0.45; Co^{3+}[B], 0.53; Zn^{2+}(A), 0.58; Zn^{2+}[B], 0.73; and O^{2-}, 1.38 and the Shannon's ionic radii[30] of Cu^{2+}(A), 0.57; Cu^{2+}-[B], 0.73; and Ni^{3+}[B], 0.56 have led to the results shown in Table 4. The more significant data are as follows:

Co_3O_4. The spinel obtained has a normal cationic distribution. The *a*, *u*, *L*(A), and *L*[B] values are in excellent agreement with data from previous studies.[31,32]

$Cu_xNi_yCo_{3-(x+y)}O_4$. In these spinels, and for the lowest $x = 0.07$ value, the best fit is obtained when all nickel atoms occupy the octahedral B positions as Ni^{3+}. All the Cu^{2+} ions occupy the tetrahedral sites. For higher values, $x = 0.29$ and 0.48, Cu^{2+} are distributed over both tetrahedral and octahedral sites, as found for $Cu_xCo_{3-x}O_4$.[33] However, the Cu^{2+} tetrahedral site occupancy is somewhat higher than the octahedral one.

$Cu_xZn_yCo_{3-(x+y)}O_4$. The best fits are obtained for the following cation distributions: Zn^{2+} always occupies the tetrahedral positions, while Cu^{2+} is distributed in both tetrahedral and octahedral sites. The cation distribution proposed for these spinels (Table 4) is in agreement with the distribution derived for $Cu_xCo_{3-x}O_4$ from neutron diffraction data (statistical distribution of Cu^{2+})[33] and for $Zn_xCo_{3-x}O_4$ (nearly normal spinel).[34]

Conclusions

Layered cobalt hydroxide nitrate $Co_2(OH)_3NO_3$ is tolerant with respect to combined isomorphic replacement of Co^{2+} by ions of two other 3d metals such as Ni^{2+}, Cu^{2+}, and Zn^{2+}, which permits preparation of single-phase ternary hydroxide nitrate precursors. Their single-step low-temperature decomposition provides a straightforward procedure for the synthesis under mild conditions of ternary spinel cobaltites that, to the best of our knowledge, cannot be prepared by a ceramic procedure. The cation distribution in the spinels satisfies the existing qualitative predictions based on crystal field calculation of the corresponding site preferences. It is also in good agreement with the distribution established from neutron diffraction studies of the binary Cu, Ni, and Zn spinel cobaltites.

Acknowledgment. The support of the Bulgarian Academy of Sciences and the Spanish CSIC, project 90BG0010, is gratefully acknowledged. Financial support by the projects MAT98-0904(CICyT) and 07N/0059/1998 (CAM) is also acknowledged.

CM990331E

(28) O'Neill, H. St. C.; Dollase, W. A. *Phys. Chem. Miner.* **1994**, *20*, 541.
(29) O'Neill, H. St. C.; Navrotsky, A. *Am. Miner.* **1983**, *68*, 181.
(30) Shannon, R. *Acta Crystallogr.* **1976**, *A32*, 751.
(31) Roth, W. L. *J. Phys. Chem. Solids* **1964**, *25*, 1.
(32) Knop, O.; Reid, K. I. G.; Sutarno; Nakagawa, Y. *Can. J. Chem.* **1968**, *46*, 3463.
(33) Petrov, K.; Krezhov, K.; Konstantinov, P. J. *Phys. Chem. Solids* **1989**, *50*, 577.
(34) Krezhov, K.; Konstantinov, P. *J. Phys: Condens. Matter* **1993**, *5*, 9287.